

# UNIVERSAL AND EFFICIENT TESTS FOR HOMOGENEITY OF MEAN DIRECTIONS OF CIRCULAR POPULATIONS

Ashis SenGupta<sup>1,2</sup> and Hemangi V. Kulkarni<sup>3</sup>

<sup>1</sup>*Indian Statistical Institute, Kolkata,* <sup>2</sup>*Augusta University,*  
*and* <sup>3</sup>*Shivaji University, Kolhapur*

*Abstract:* We develop an efficient test for the homogeneity of the mean directions of several independent circular populations (ANOMED) that can be universally implemented. Current tests for ANOMED are available only for highly concentrated and/or large groups. Thus, we fill the gap for a usable test under highly dispersed and/or small to medium-sized groups. Focusing on the popular von Mises distribution, a simple and elegant test statistic is derived under homogeneous concentrations across groups. The hurdle of the non-location-scale nuisance parameter  $\kappa$  is overcome by adopting a new approach based on the integrated likelihood ratio test (ILRT). Furthermore, a second-order-accurate asymptotic chi-square distribution is established for the ILRT. Notably, the test outperforms existing tests for small to moderate-size and highly dispersed (small  $\kappa$ ) groups, which is precisely the parametric region of prime concern, where previous tests were either unusable or unsatisfactory. The test also outperforms the popular Watson–Williams test for highly concentrated small groups, and shows competitive performance compared with that of its best competitors and, hence, can be universally used in all situations. The ILRT extends naturally under heterogeneous concentrations, and is amenable to elegant generalizations to a rich variety of circular populations and to higher dimensions (i.e., to distributions on the sphere and hypersphere). Lastly, the test is illustrated using three real-life data sets.

*Key words and phrases:* Batschelet distribution, circular ANOVA, circular normal distribution, generalized von Mises distribution, integrated likelihood ratio tests, Watson-Williams test.

## 1. Introduction

Observations on angular movements or displacements and on directional propagations on a plane commonly constitute circular data. Strictly periodic occurrences, rhythmic activities, and compositional data may also fall within this category. Analytically, any data that can be mapped uniquely onto the circumference of a unit circle is defined as circular data. Analyses of such data differ markedly from those for linear data, owing to the disparate topologies between

the line and the circle. Refer to Mardia and Jupp (2000)(MJ) and Jammalamadaka and SenGupta (2001) (JS), and Fisher (1993) for further details.

Often, a situation demands a comparison of the mean directions of several independent populations; see Lozano (2016) and Shay et al. (2016) for recent applications. We refer to such a comparison as an analysis of mean directions (ANOMED). The present work develops efficient test procedures for an ANOMED under the popular von Mises (vM) or circular normal distribution.

An overview of the existing literature on ANOMED for vM (see Section 2) reveals that tests are available either for highly concentrated data (Watson and Williams (1956)) or for large samples (e.g., see the corresponding likelihood ratio test (LRT) in MJ). Under similar conditions, useful references on ANOMED include Beran and Fisher (1998) for bootstrap-based pairwise comparisons between mean directions, Larsen, Blaesild and Sorensen (2002) for improved likelihood ratio-based tests for the two-sample problem, and SenGupta and Roy (2011) for an analysis of deviance-based approach with vM and wrapped Cauchy distributions.

In the present scenario, it appears that for vM, no satisfactory tests exist for highly dispersed data (small concentration parameter) and small to moderate group sizes, despite the frequency with which such data occur in diverse areas of applied research. An example attesting to this fact is also given in this paper. The present work attempts to fill this gap by developing an integrated likelihood ratio test (ILRT), which eliminates the nuisance concentration parameter  $\kappa$  by integrating it out of the likelihood function using a suitably chosen weight function. Then, a second-order-accurate asymptotic chi-square distribution for the ILRT is derived. Extensive simulation-based comparisons show that the proposed test outperforms its competitors under small concentration parameters, and performs as equally well as its best competitors otherwise, rendering it universally applicable. Tests for ANOMED under generalized von Mises (GvM) and Batschelet distributions are outlined. A version of the ILRT for heterogeneous concentrations across groups is also developed. The new test is illustrated using real data sets.

The remainder of the paper proceeds as follows. Section 2 summarizes the existing methods. The proposed ILRT, its asymptotic distribution, and its performance assessment in comparison to its competitors are addressed in Section 3. Section 4 develops the analogue of the ILRT under unequal concentrations, derives its asymptotic distribution, and discusses its extensions to other distributions. Section 5 exemplifies the use of the ILRT using real data sets, relative

to the existing tests. Section 6 concludes the paper.

## 2. Preliminaries and Review

### 2.1. Preliminaries

The angular observations  $\theta_{ij}$ , for  $i = 1, \dots, p$ ,  $j = 1, \dots, n_i$ ;  $\theta_{ij} \in (0, 2\pi]$ , are assumed to follow the vM or circular normal distribution, with pdf

$$f(\theta_{ij}) = \frac{1}{2\pi I_0(\kappa)} \exp\{\kappa \cdot \cos(\theta_{ij} - \mu_i)\},$$

where  $\kappa > 0$  is the concentration parameter,  $\mu_i \in (0, 2\pi]$  is the mean direction for the  $i$ th group, and  $I_0(\kappa)$  is the modified Bessel function of the first kind with order zero. The maximum likelihood estimate (MLE) of the  $i$ th group mean direction  $\mu_i$  is given by  $\theta_{i.}$ , the quadrant-specific sample mean direction (Jammalamadaka and SenGupta (2001, p.13)). Let  $C_i = \sum_{j=1}^{n_i} \cos(\theta_{ij})$ ,  $S_i = \sum_{j=1}^{n_i} \sin(\theta_{ij})$ , and  $n = \sum_{i=1}^p n_i$ . The length of the resultant vector for the  $i$ th group in its two equivalent forms is  $R_i = (C_i^2 + S_i^2)^{\frac{1}{2}} = \sum_{j=1}^{n_i} \cos(\theta_{ij} - \theta_{i.})$ . The MLE  $\hat{\kappa}_1$  of  $\kappa$  is a solution of the equation  $A(\hat{\kappa}_1) = (\sum_{i=1}^p R_i)/n$ , where  $A(\cdot) = I_1(\cdot)/I_0(\cdot)$ .

The mean direction  $\theta_{..}$  of the combined sample and its resultant length  $R$  are obtained similarly, based on the combined sample, by replacing  $C_i$  and  $S_i$  with  $C = \sum_{i=1}^p C_i$  and  $S = \sum_{i=1}^p S_i$ , respectively. The standardized lengths for the  $i$ th group and the combined sample are given by  $\bar{R}_i = R_i/n_i$  and  $\bar{R} = R/n$ , respectively.

Here we test  $H_0 : \mu_1 = \dots = \mu_p$ , versus at least one inequality in mathematical terms. Under  $H_0$ , the MLE of  $\mu_0$  is  $\theta_{..}$ , whereas that of  $\kappa$  is  $\hat{\kappa}_0$ , where  $A(\hat{\kappa}_0) = \bar{R}$ . The existing tests for ANOMED under vM are described below.

### 2.2. Existing methods

The literature addresses the problem of ANOMED for a high concentration (large  $\kappa$ ) or for large sample sizes. As a result, four corresponding types of tests exist (see e.g., Mardia and Jupp (2000, Chap. 10)): two high-concentration tests, namely the Watson–Williams (WW) and Harrison, Kanji, Gadsden (HKG) tests, and two LRT-based large-sample tests.

1. WW test with a multiplicative correction:

$$T_{WW} \equiv \left(1 + \frac{3}{8\hat{\kappa}_0}\right) \frac{(n-p)SS_B}{(p-1)SS_W} \sim F_{p-1, n-p},$$

for large  $\kappa$ , where  $SS_W = 2\kappa(n - \sum_{i=1}^p R_i)$  and  $SS_B = 2\kappa(\sum_{i=1}^p R_i - R)$ . The corrective adjustment  $(1 + 3/(8\hat{\kappa}_0))$  is suggested by Stephens (1972), and is recommended for  $\hat{\kappa}_0 > 2$ .

2. HKG with a multiplicative correction:

$$T_{HKG} \equiv \left(1 - \frac{1}{5\hat{\kappa}_0} - \frac{1}{10\hat{\kappa}_0^2}\right) \frac{(n-p)SS_{Tr}}{(p-1)SS_E} \sim F_{p-1, n-p},$$

for large  $\kappa$ , where  $SS_{Tr} = (\sum_i n_i \bar{R}_i^2 - n \bar{R}_{..}^2)$  and  $SS_E = (n - \sum_i n_i \bar{R}_i^2)$ .

3. LRT:

$$T_{LRT} = 2 \left[ n \{ \log I_0(\hat{\kappa}_0) - \log I_0(\hat{\kappa}_1) \} + \hat{\kappa}_1 \sum_i R_i - \hat{\kappa}_0 R \right] \stackrel{a}{\sim} \chi_{p-1}^2.$$

4. Anderson and Wu test (AW):

Anderson and Wu (1995) suggested using  $\hat{\kappa}_0$  in place of  $\hat{\kappa}_1$  in  $T_{LRT}$ , with the same asymptotic chi-square distributional assumption.

Here  $\stackrel{a}{\sim}$  refers to an asymptotic distribution.

Although highly dispersed and/or small to medium-sized groups are often encountered in practice, existing tests either are not applicable or fail to perform well. See Section 3.3 for a rigorous discussion of this point. This study seeks to fill this gap. To do so, we develop a test that should work uniformly in all situations. Here, we eliminate the nuisance concentration parameter to improve the quality of the LRT-based tests.

In the next section, we develop an integrated likelihood test, ILRT, for ANOMED, and derive its second-order asymptotic chi-square distribution. A detailed assessment of the test reported in Section 3.3 reveals uniformly satisfactory performance. Furthermore, the proposed test outperforms other tests in the aforementioned regions.

### 3. The Proposed ILRT

#### 3.1. The integrated likelihood ratio approach

Consider a likelihood function  $L(\boldsymbol{\psi}, \boldsymbol{\lambda})$ , where  $\boldsymbol{\psi}$  is the parameter of interest, and  $\boldsymbol{\lambda} \in \boldsymbol{\Lambda}$  is the nuisance parameter. The likelihood inference about  $\boldsymbol{\psi}$  is often based on a pseudo-likelihood function  $L_{\boldsymbol{\psi}}$ , obtained by eliminating  $\boldsymbol{\lambda}$  in a suitable way, which maintains the properties similar to those of a regular likelihood. The

most popular is the profile likelihood (PL)  $L_p$  (and its modifications), which replaces the nuisance parameter with  $\hat{\lambda}_\psi$ , the maximizer of  $L$  with respect to  $\lambda$  under fixed  $\psi$ . However the PL has several drawbacks. First, Maximizing over  $\lambda$  can be challenging in the case of a large number of nuisance parameters. See also example 2 (yielding '0' as the PL-based MLE for the population variance under every observable data set), example 3 (yielding a strange likelihood, rapidly growing to  $\infty$  as the parameter  $\theta \rightarrow \infty$  or  $-\infty$ , depending on the sign of the sample mean), and example 4 (PL is nearly useless for inferences, being nearly constant over a huge range of the parameter space) of Berger, Liseo and Wolpert (1999) for other undesirable situations.

Given this background, the "averaging" effect produced by an integrated likelihood (IL) is expected to produce a better summary of the original likelihood than that of the "maximization" in the profile likelihood. Refer to Berger, Liseo and Wolpert (1999) for a critical discussion about pseudo likelihoods, where the use of IL is strongly recommended for several reasons, including accounting for nuisance parameter uncertainty. For further insights, refer to Kalbfleisch and Sprott (1970) and Liseo (1993), among others. An IL is of the form

$$\bar{L}(\psi) = \int_{\Lambda} L(\psi, \lambda) \cdot \Pi(\lambda|\psi) d\lambda. \quad (3.1)$$

Here,  $\Pi$  is a nonnegative weight function on  $\Lambda$ , making the above integral convergent for every fixed  $\psi$ .

Because  $\bar{L}$  depends only on the data and the parameter of interest  $\psi$ , it can be used like a standard likelihood function for all likelihood-based inference procedures. However, choosing  $\Pi$  to produce good inference procedures is an important issue, one that remains unresolved under multiple parameters of interest, as in the present inference problem of ANOMED.

Effective IL-based inference procedures are considered by Chamberlain (2007), Ghosh et al. (2006), and Malley et al. (2003), among others. Severini (2007, 2010, 2011) gives a thorough development of inference procedures about a scalar parameter of interest  $\psi$ , particularly when the nuisance parameters  $\lambda$  and the scalar parameter of interest  $\psi$  are orthogonal; that is, the expected values of the mixed derivatives of the log likelihood function with respect to  $\lambda$  and  $\psi$  are zeros. In this case, the impact of the choice of  $\Pi$  is quite low when  $\Pi$  does not depend on  $\psi$ , in moderate to large samples. However, parameter orthogonality is not a necessary condition for the ILRT to produce good inference procedures.

In the following, the ILRT statistic is developed for ANOMED under equally

dispersed vM distributions. Its second-order asymptotic chi-square distribution is derived. An extensive simulation-based assessment of its performance is carried out in Section 3.3.

### 3.2. ILRT under equal concentration parameters

Referring to section 2.1, the likelihood function is

$$L(\boldsymbol{\mu}|\boldsymbol{\theta}, \kappa) = \frac{1}{I_0(\kappa)^n} \exp \left[ \kappa \left\{ \sum_{i=1}^p \sum_{j=1}^{n_i} (\cos(\theta_{ij} - \mu_i)) \right\} \right], \kappa > 0, \mu_i \in [0, 2\pi), \forall i.$$

Here,  $\boldsymbol{\theta} = (\theta_{11}, \theta_{12}, \dots, \theta_{1n_1}, \dots, \theta_{p1}, \dots, \theta_{pn_p})$  is the vector of all observations, and  $\boldsymbol{\psi} = \boldsymbol{\mu} = (\mu_1, \dots, \mu_p)$  is the vector parameter of interest. The choice of prior,

$$\Pi(\kappa) = I_0(\kappa)^n \exp(-n\kappa) \kappa^{a_n-1}, \kappa > 0, \quad (3.2)$$

is motivated by its success in attaining a simple closed form of the IL, after eliminating the normalizing constant  $I_0(\kappa)^{-n}$  and choosing the exponent  $\exp(-n\kappa)$  to make the resulting integral convergent for all observed data sets and mean directions. Nevertheless, we would like to keep it free from the parameter of interest  $\boldsymbol{\psi}$ . This choice, together with the parameter orthogonality between  $\boldsymbol{\psi}$  and  $\kappa$ , provides the resulting ILRT with the desired second-order properties, as seen in the proof of Theorem 1 (see also Severini (2007)). The term  $\kappa^{a_n/2-1}$ , the exponent of which produces the scaling factor  $a_n$  in the resulting ILRT statistic, is used to attain a nondegenerate limiting distribution. In line with the Welch–Satterthwaite technique, an initial guess of  $a_n = n - 1$  is based on matching the simulated means (first moments) of  $T_{ILRT}$  to  $p - 1$ , the expected values of the desired asymptotic  $\chi^2$  distribution, under a large group size and large  $\kappa$ . More precisely,  $n_1 = 100$  and  $\kappa = 15$  were taken as representatives of large group sizes and large concentrations, respectively. Then, the ratio of  $p - 1$  to the simulated mean (based on 500,000 simulations) of the RHS of (3.3), excluding the  $(n - 1)$  term (which is the simulated value of the  $a_n$  term), was regressed on the total sample size  $n$  for  $p = 2(1)8$ . The value of  $a_n$  was further tuned for its modest dependence on the unknown  $\kappa$  using multiplicative adjustments, as suggested in section A.1 of Appendix A. Finally, integrating  $L\Pi$  over  $\kappa \in (0, \infty)$  results in the integrated likelihood function

$$\bar{L}(\boldsymbol{\mu}|\boldsymbol{\theta}) \propto \left[ n - \sum_{i=1}^p \sum_{j=1}^{n_i} \cos(\theta_{ij} - \mu_i) \right]^{-(n-1)/2}.$$

The integrated MLEs obtained by maximizing  $\bar{L}$  with respect to  $\boldsymbol{\mu}$  under the null and the alternative hypotheses coincide with the usual ones,  $\bar{\psi}_0 = \bar{\mu}_0 = \theta_.$  and  $\bar{\boldsymbol{\psi}}_1 = \bar{\boldsymbol{\mu}}$ ;  $\bar{\mu}_i = \theta_{i.}$ , for  $i = 1, \dots, p$ , respectively (see Section 2.1). The resulting IL ratio is

$$\bar{\lambda} = \frac{\sup_{\Theta_0} \bar{L}(\boldsymbol{\mu}|\boldsymbol{\theta})}{\sup_{\Theta_1} \bar{L}(\boldsymbol{\mu}|\boldsymbol{\theta})} = \left[ \frac{n - \sum_{i=1}^p R_i}{(n - R)} \right]^{(n-1)/2},$$

where  $\Theta_1 = \{\boldsymbol{\mu} : \mu_i \in (0, 2\pi], i = 1, \dots, p\}$ , and  $\Theta_0 = \{\mu(1, 1, \dots, 1)_{p \times 1}, \mu \in (0, 2\pi] \}$  is the subset of  $\Theta_1$  comprising all components of  $\boldsymbol{\mu}$  equal to  $\mu$ . The proposed ILRT statistic  $-2 \log \bar{\lambda}$  is

$$T_{ILRT} = -(n - 1) \log \left[ \frac{n - \sum_{i=1}^p R_i}{n - R} \right]. \tag{3.3}$$

The asymptotic  $\chi^2$  distribution of  $T_{ILRT}$  is stated in Theorem 1.

Throughout this paper, the parameter space for  $\kappa$  is assumed to be  $(0, \infty)$ . (The case  $\kappa = 0$  is excluded, being a uniform distribution over  $[0, 2\pi)$ ).

**Theorem 1.** *The asymptotic distribution of  $T_{ILRT}$  is  $\chi_{p-1}^2$ .*

*Proof of Theorem 1.* Let  $C(\boldsymbol{\psi}) = \sum_{i=1}^p \sum_{j=1}^{n_i} \cos(\theta_{ij} - \mu_i)$ . Writing  $L(\kappa)$  for  $L(\kappa|\boldsymbol{\mu}; \boldsymbol{\theta})$ , let

$$\begin{aligned} h(\kappa) &= -\frac{1}{n} \log(L(\kappa)) \\ &= \log(I_0(\kappa)) - \frac{\kappa}{n} C(\boldsymbol{\psi}). \end{aligned}$$

It is easily seen that the partial derivatives of  $h$  with respect to  $\kappa$  are

$$\begin{aligned} h'(\kappa) &= -\frac{C(\boldsymbol{\psi})}{n} + A(\kappa); \\ h^{(j)}(\kappa) &= A^{(j-1)}(\kappa); \quad j = 2, 3, \dots, \end{aligned} \tag{3.4}$$

where  $A^{(j)}$  is the  $j$ th derivative of  $A(\kappa)$  with respect to  $\kappa$ .

First, consider the case of large concentrations,  $\kappa > 1$ . Here,  $A(\kappa)$  and its  $j$ th derivative can be shown to be piece-wise well approximated to  $O(10^{-3})$  by

$$\begin{aligned} A(\kappa) &\approx c + \frac{b}{\kappa}; \\ A^{(j)} &\approx b (-1)^{(j)} \frac{j!}{\kappa^{j+1}}; \quad j = 1, 2, \dots \end{aligned} \tag{3.5}$$

The constant  $c$  varies slightly across the pieces, and is almost zero for large

concentrations, whereas the slope  $b$  is very close to 2. See Table 2 of Section A.2, Appendix A, for details. See also A.13 of Appendix 1 of JM for another approximation. The Taylor expansion of  $h$  about  $\hat{\kappa}_\psi \equiv \hat{\kappa}$ , with equations (3.4) and (3.5), and the fact that  $h'(\hat{\kappa}) = 0$ , yield the following:

$$nh(\kappa) = -\log(L(\hat{\kappa})) + \frac{1}{2}A'(\hat{\kappa})u^2 + \left\{ \frac{-2u^3}{\sqrt{n}3(\hat{\kappa})^3} + \frac{2u^4}{n4(\hat{\kappa})^4} \right\} + r_n(u),$$

where  $u = \sqrt{n}(\kappa - \hat{\kappa})$  and  $r_n(u)$  is  $O(n^{-1.5})$ .

Note that the prior  $\Pi$  is continuously differentiable. Then, applying the expansion of  $e^{-x}$  to the third term (inside the curly bracket) and using Taylor's expansion of  $\Pi(\kappa)$  about  $\hat{\kappa}$  gives

$$\begin{aligned} L(\kappa).\Pi(\kappa) &= \exp\{-nh(\kappa)\}\Pi(\kappa) \\ &= \frac{L(\hat{\kappa})}{\sqrt{n}|A'(\hat{\kappa})|} \cdot \sqrt{n|A'(\hat{\kappa})|} \exp\left\{-\frac{A'(\hat{\kappa})u^2}{2}\right\} \\ &\cdot \left\{ 1 - \left[ \frac{-2u^3}{3\sqrt{n}(\hat{\kappa})^3} + \frac{2u^4}{4n(\hat{\kappa})^4} \right] + \frac{1}{2} \left[ \frac{-2u^3}{3\sqrt{n}(\hat{\kappa})^3} + \frac{2u^4}{4n(\hat{\kappa})^4} \right]^2 + R_{1n}(\kappa, \hat{\kappa}) \right\} \\ &\left\{ \Pi(\hat{\kappa}) + \frac{1}{\sqrt{n}}\Pi'(\hat{\kappa})u + \frac{1}{2n}\Pi''(\hat{\kappa})u^2 + \frac{1}{6n\sqrt{n}}\Pi^{(3)}(\hat{\kappa})u^3 + R_{2n}(\kappa, \hat{\kappa}) \right\}, \end{aligned} \tag{3.6}$$

where  $R_{1n}$  and  $R_{2n}$  are of  $O(n^{-2})$ . First compute the product of the two bracketed terms on the RHS of (3.6), and then multiply the resulting terms by  $\sqrt{n}|A'(\hat{\kappa})|\exp\{(-1/2)A'(\hat{\kappa})u^2\}$ , which is proportional to a normal density with mean zero and standard deviation  $A'(\hat{\kappa})^{-1/2}$ . Next, integrate term by term with respect to  $\kappa$ , and note that  $d\kappa = \sqrt{n} du$ . Then, on the RHS of (3.6), the integrals involving powers of  $u$  are proportional to the raw moments of a normal distribution with mean zero and standard deviation  $A'(\hat{\kappa})^{-1/2}$ . The use of (3.5) with the approximation  $b \approx 2$  makes the  $(2j)$ th raw moment  $\mu'_{2j} = 2\hat{\kappa}^{2j}(2j)!/(2^j j!2^j)$ , a constant multiple of  $\hat{\kappa}^{2j}$ , while the odd order moments vanish. Ignoring the  $O(n^{-2})$  terms, the RHS of (3.6) becomes

$$\begin{aligned} \int L(\kappa).\Pi(\kappa)d\kappa &\propto L_A(\hat{\kappa}) \left\{ \Pi(\hat{\kappa}) + \frac{\Pi''(\hat{\kappa})\mu'_2}{2n} + \frac{\Pi'(\hat{\kappa})\mu'_4}{3n\hat{\kappa}^3} \right. \\ &\left. - \frac{\Pi(\hat{\kappa})\mu'_4}{2n\hat{\kappa}^4} + \frac{\Pi(\hat{\kappa})\mu'_6}{9n\hat{\kappa}^6} + O(n^{-2}) \right\}, \end{aligned} \tag{3.7}$$

where  $L_A(\boldsymbol{\psi}) \propto L(\boldsymbol{\psi}, \hat{\kappa}_{\boldsymbol{\psi}}) |l_{\kappa\kappa}|_{\{\kappa=\hat{\kappa}\}}^{-1/2}$  is the Cox and Reid (1987) adjusted profile likelihood,  $|l_{\kappa\kappa}|_{\{\kappa=\hat{\kappa}\}} = nA'(\hat{\kappa})$ , where  $l_{\kappa\kappa}$  is the second-order partial derivative of the log likelihood  $l$  with respect to  $\kappa$ . Furthermore, from (3.5),  $\Pi'(\kappa) \approx n\Pi(\kappa)(2.5/\kappa - \theta)$  and  $\Pi''(\kappa) \approx \Pi(\kappa)n^2(2.5/\kappa - \theta)^2$ , where  $\theta = 1 - c$  is close to one (for large  $\kappa$ ,  $c$  is very close to zero, see Table 2, Section A.2, Appendix A for more details). Consequently, ignoring the  $O(n^{-2})$  terms, the above observations yield

$$\bar{L}(\boldsymbol{\psi}) = \int L \cdot \Pi(\kappa) d\kappa \propto L_A(\hat{\kappa}) \cdot \Pi(\hat{\kappa}) g(\hat{\kappa}) \{1 + O(n^{-1.5})\}, \quad (3.8)$$

where, for every fixed  $n$ , both  $g$  and  $\Pi$  are finite and continuous in  $\kappa$ . Taking the logarithms and denoting the log likelihoods by  $l$  yields

$$\bar{l}(\boldsymbol{\psi}) = l_A(\boldsymbol{\psi}) + \log(\Pi(\hat{\kappa}_{\boldsymbol{\psi}})) + \log(g(\hat{\kappa}_{\boldsymbol{\psi}})) + \log(\{1 + O(n^{-1.5})\}).$$

Recall from Section 2.1 that  $\bar{\boldsymbol{\psi}}_1 = \hat{\boldsymbol{\mu}}$ ,  $\bar{\psi}_0 = \hat{\mu}_0$ , are the usual MLEs of  $\boldsymbol{\mu}$ , whereas those of  $\kappa$  are  $\hat{\kappa}_1 = \sup_{\boldsymbol{\psi}} \hat{\kappa}_{\boldsymbol{\psi}}$  and  $\hat{\kappa}_0$  under  $H_i$ , for  $i = 1, 0$ . The resulting ILRT statistic is

$$-2 \log \bar{\lambda} = -2(l_A(\hat{\boldsymbol{\mu}}) - l_A(\hat{\mu}_0)) + 2 \log \left( \frac{\Pi(\hat{\kappa}_1)}{\Pi(\hat{\kappa}_0)} \right) + 2 \log \left( \frac{g(\hat{\kappa}_1)}{g(\hat{\kappa}_0)} \right) + O_P(n^{-1.5}). \quad (3.9)$$

Note that  $\Pi$  (by our choice) and  $g$  depend on the parameter of interest  $\boldsymbol{\psi}$  only through  $\kappa_{\boldsymbol{\psi}}$ . Additionally,  $E(\partial^2 l / \partial \kappa \partial \mu_i) = 0$ , for  $i = 1, \dots, p$ , (see MJ) so that the nuisance parameter  $\kappa$  is orthogonal to the parameter of interest  $\boldsymbol{\psi} = \boldsymbol{\mu}$ . Consequently,  $\hat{\kappa}_{\boldsymbol{\psi}}$  is less sensitive to the variation in  $\boldsymbol{\psi}$  under the null and the alternative hypotheses (see Section 2.2, result (iv) of Cox and Reid (1987)). Additionally, both  $\hat{\kappa}_1$  and  $\hat{\kappa}_0$  being consistent for the same parameter  $\kappa$ ,  $|\hat{\kappa}_1 - \hat{\kappa}_0| = O_P(n^{-1})$ . Together with the continuity of  $\Pi$  and  $g$ , this makes the terms  $\log(\Pi(\hat{\kappa}_1)/\Pi(\hat{\kappa}_0))$ ,  $\log(g(\hat{\kappa}_1)/g(\hat{\kappa}_0))$ , and the middle term in equation (3.9) all  $O_P(n^{-1})$ . These arguments finally lead to

$$T_{ILRT} = -2 \log \bar{\lambda} = -2(l_A(\hat{\boldsymbol{\mu}}_1) - l_A(\hat{\mu}_0)) + O_P(n^{-1}),$$

where the computational form is given in equation (3.3). The asymptotic distribution of  $T_{ILRT}$  is the same as that of the adjusted profile log likelihood ratio, namely  $\chi_{p-1}^2$ . The approximations involving  $\kappa$  in (3.5) (leading to the  $\chi^2$  distributional approximation) are very sharp for large  $\kappa$ , say  $\kappa > 9$ , but not so for  $\kappa < 9$ . A slight fine-tuning in the form of subtle multiplicative adjustments is given in Section A.1 of Appendix A. This is based on the piece-wise partition of

the approximation of  $A(\kappa)$ , and significantly improves the  $\chi_{p-1}^2$  approximation for this case.

The case of a small concentration can be dealt with in a similar way by noting that, in this case, the function  $A(\kappa)$  can be well approximated by  $0.107 + 0.46\kappa$ , with a maximum deviation of order  $10^{-3}$ , for  $\kappa \in (0.1, 0.9)$ . For  $\kappa < 0.1$ , the circular uniform distribution is recommended. Here, the derivatives of  $A(\kappa)$ , and hence of  $h(\kappa)$ , of order greater than one all vanish, simplifying the RHS of (3.6) to a great extent. However, in this region, the estimates of  $\kappa$  are likely to be more sensitive. Moreover, the derivatives of  $\Pi$  involve reciprocals of  $\hat{\kappa}$ . Hence, the RHS of (3.9) is expected to be more unstable, resulting in large observed sizes, as shown in a simulation study (not discussed here, for brevity). This problem was handled by ad-hoc multiplicative adjustments to the resulting ILRT, as developed in Section A.1 of Appendix A.

**Remark 1.**

- (i) The aforementioned multiplicative adjustments controlled the sizes of the resulting tests very well, without affecting its power function, as can be seen in the simulation study reported in the next subsection. These adjustments are used throughout the remainder of this paper, including the performance assessment in Section 3.3 and the real-data analysis in Section 5, and are strongly recommended in practice.
- (ii) Although the results from Cox and Reid (1987) under parameter orthogonality used here were originally developed for a real-valued parameter of interest, these remain valid for a vector-valued parameter of interest, as long as the orthogonality between the vector parameter of interest and the nuisance parameters holds, as in our case.

The next subsection attempts an extensive simulation-based comparison between the ILRT and the existing tests.

**3.3. Performance assessment**

A study based on 50,000 simulated observations from vM distributions on the circle is conducted to compare the size and power of the ILRT with those of the two high-concentration tests and the two likelihood-based tests reported in Section 2.2. A large number of situations are considered to form a fair representation of practical scenarios: group sizes  $n_1 = 15, 20, 30, 40, 60$ ; concentration parameters  $\kappa=0.25, 0.3(0.04)0.44; 0.45, 0.5(0.1)1.5; 2(1)10; 15, 20,$

40, 70, 100; and number of groups  $p = 2(1)8$ . The level of significance was fixed at the commonly used 5% level. Note that the parametric space under  $H_1$  for the mean vectors  $\boldsymbol{\mu}$ ,  $\Theta_1 = [0, 2\pi)^p$ , is  $p$ -dimensional, whereas the power function is a surface in  $p + 1$  dimensions. A comparative study of the power surfaces of several tests in  $p + 1$  dimensions is challenging, particularly when  $p$  is large, and may lack visual clarity. To avoid such complications, and noting the periodic nature of  $\mu_i$ , such that the farthest components of  $\boldsymbol{\mu}$  can be at most  $\pi$  distance from each other, a systematic subset of  $[0, 2\pi)^p$  is selected,  $\{\boldsymbol{\mu} = h/(p-1) \cdot (0, 1, \dots, p-1); h = 0 (\pi/6) \pi\}$ . Here, we scale the vector  $(0, 1, \dots, p-1)/(p-1) \in \Theta_1$  by a real positive number  $h$ , varying  $h$  over the grid  $\{0 (\pi/6) \pi\}$ , for the computation of powers so that the resulting collection of powers can be plotted against  $h$  as a function in two dimensions, henceforth referred to as "the power function". This enables a visually clear picture of the power functions and a clearer comparison of the tests.

(A) *Size performance*

Note that the case of  $h = 0$  corresponds to the observed sizes of the respective tests. Box plots of the simulated sizes for the aforementioned four tests and the ILRT are shown in Figure 1. A careful assessment of the simulated sizes based on various graphical tools (not reported here, for brevity) revealed the following prominent features:

- i) The large outliers in the box plots for WW basically emerged from small concentrations ( $\kappa < 1$ ). The magnitude of outliers increased with the number of groups ( $p$ ), but group sizes ( $n_1$ ) had almost no impact. This behavior is consistent with the role of the large concentration behind WW's construction.
- ii) The observed sizes of the other large concentration test, HKG, revealed a similar impact of  $\kappa$  and  $p$  (but not of  $n_1$ ), albeit in the opposite directions; that is, tiny sizes (often very close to zero) increased with  $\kappa$  and stabilized to the desired level after  $\kappa$  became as large as 40. This, in turn, resulted in reduced power, as revealed by Figures 2–5.
- iii) The whiskers and outliers for LRT emerged under all three factors: small  $\kappa$ , large  $p$ , and small  $n_1$ . Under small concentrations, the group sizes required to stabilize the sizes around the desired level 0.05 were as large as 60. For large concentrations, the convergence was relatively fast.
- iv) AW exhibited a pattern similar to LRT, but in the opposite direction, as

HKG did.

Clearly, based on the size performance, WW and LRT were practically unusable under small concentrations and/or small groups.

(B) *Power performance*

To ensure a fair comparison between the tests, two versions of the power function were simulated:

- (I) For an unbiased comparison among all available tests, the normalized power function was generated by multiplying the original uncorrected tests by the ratio of the respective theoretical  $\chi^2$  or  $F$  quantile to the simulated quantile of the uncorrected statistics, for the particular parameter combination under concern. This guaranteed the size of all cases to be exactly 0.05, making the power comparison unbiased. Figure 2 presents the gain in power over other tests by the ILRT, under the normalized power function at  $h = \pi$  as a function of  $\kappa$  for small concentrations at various combinations of  $p$  and  $n_1$ . Figure 3 displays similar plots for very small concentrations ( $\kappa = 0.25$  and  $0.3$ ) as a function of  $p$ .
- (II) Viewing AW as the "size-corrected" version of LRT, the actual (non-normalized) power functions of AW and HKG were compared with the ILRT. Representative power functions for the  $p = 2$  and  $p = 8$  groups are presented in Figures 4–5 for small concentrations, and in Figures 6–7 for large concentrations. WW and LRT are unusable owing to their large sizes under small concentrations; thus, their power functions are not included in Figures 4 and 5, whereas Figures 6 and 7 include all tests.

Both the normalized and non-normalized power functions showed similar patterns in excess power (gain) attained by the ILRT. A careful observation of Figures 2–7 strongly supports the following points.

***Small concentrations:***

- i) As targeted, a notable gain for the ILRT was observed over its competitors, AW and HKG, under small concentrations, namely  $\kappa < 1$ , and more prominently for  $\kappa < 0.5$  (see Figures 2–5).
- ii) For very small  $\kappa$ , the gain was increasing with the number of groups ( $p$ ) for fixed values of other parameters (see Figure 3).
- iii) For two groups and/or  $\kappa < 0.5$ , the gain over AW was uniformly more than that over HKG, even under large group sizes (Figure 3 and first row of

Figure 2). However, this behavior reversed for large numbers of groups and  $0.5 < \kappa < 1$ . Under large group sizes and  $\kappa$  in the neighbourhood of one, the three tests performed almost equally (last two rows of Figure 2).

***Large concentrations:***

- iv) Under medium  $\kappa$  ( $1 < \kappa < 2$ ) and very small group sizes, the likelihood-based tests surpassed WW, with the gain increasing with  $p$  (first row of Figures 6–7).
- v) Under large concentrations and large group sizes, all tests, including the regular LRT, performed almost equally well (Figure 7). However, for two groups, the power of AW declined in the farthest region from the null hypothesis, that is at  $h = \pi$ , particularly under large concentrations and small group sizes (Figure 6).

**Remark 2.**

- (i) Because the unadjusted versions of the ILRT and WW are functionally related, namely  $ILRT = (n - 1) \log(WW - 1)$ , the normalized power functions of the two are almost the same; thus, WW is not included in Figures 2–3. However their distributions, and hence cut-off points, are different. As noted above, under small concentrations, WW yields large sizes, making it practically unusable.
- (ii) The main benefit of the ILRT was evident under small concentrations and/or small group sizes, as desired. The ILRT not only improved over LRT and AW, but was also superior to all other tests in this scenario. It compared well in all other cases to the best performers and, hence, can be uniformly used under all situations, irrespective of the magnitude of the observed values of  $\kappa$  and the group sizes.

The next section discusses an extension of the ILRT to heterogeneous groups. An extension to GvM and the Batschelet distributions is also outlined. Note that our approach can be adapted easily and elegantly for a generalization of ANOMED to distributions on hyper-spheres.

## 4. Extensions of ILRT to Other Cases

### 4.1. ILRT under unequal concentration parameters

The  $p$  groups may follow vM distributions with differing concentration parameters. The setup is similar to the that in Section 3.2, except that now  $\theta_{ij} \sim$

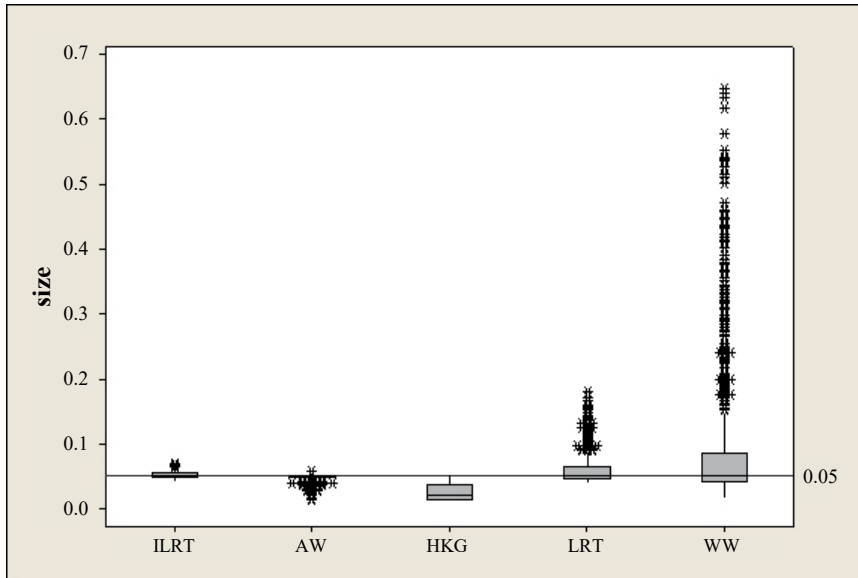


Figure 1. Box plots of simulated sizes of all tests for the parametric combinations reported in Section 3.3.

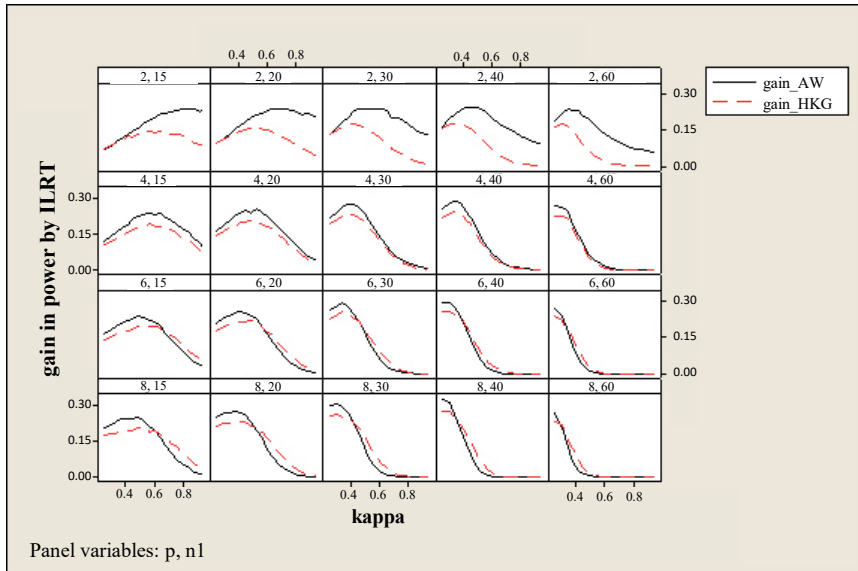


Figure 2. Gain in normalized power by ILRT over AW and HKG vs.  $\kappa$  ( $< 1$ ) for various group sizes ( $n_1$ ) and number of groups ( $p$ ). Panel headings are values of the pairs  $p, n_1$ .

von-Mises  $(\mu_i, \kappa_i)$ , for  $i = 1, \dots, p$ . The likelihood function is given by

$$L^*(\boldsymbol{\mu}, \boldsymbol{\kappa} | \boldsymbol{\theta}) = \prod_{i=1}^p L_i, \quad L_i = \frac{1}{I_0(\kappa_i)^{n_i}} \exp \left[ \kappa_i \left\{ \sum_{j=1}^{n_i} \cos(\theta_{ij} - \mu_i) \right\} \right].$$

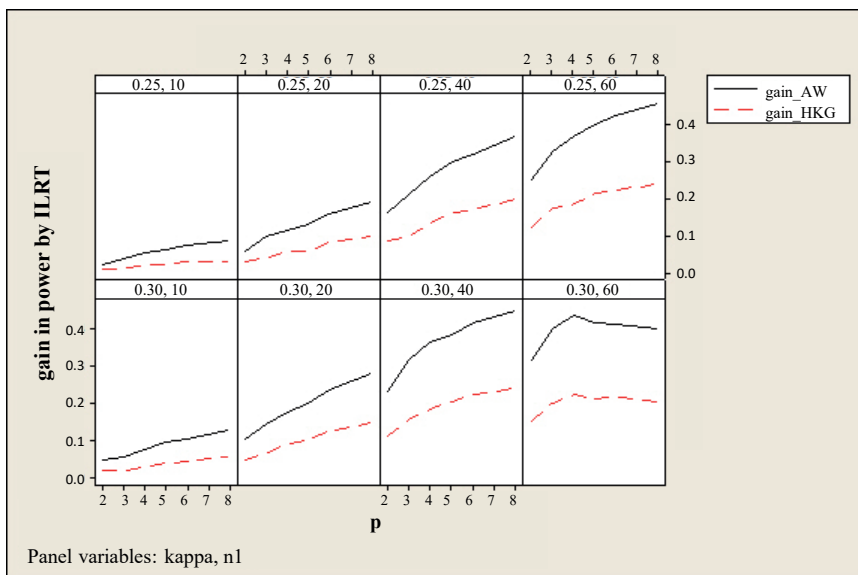


Figure 3. Gain in normalized power by ILRT over AW and HKG vs.  $p$  for various group sizes ( $n_1$ ) and concentrations  $\kappa = 0.25$  and  $0.3$ . Panel headings are values of the pairs  $\kappa, n_1$ .

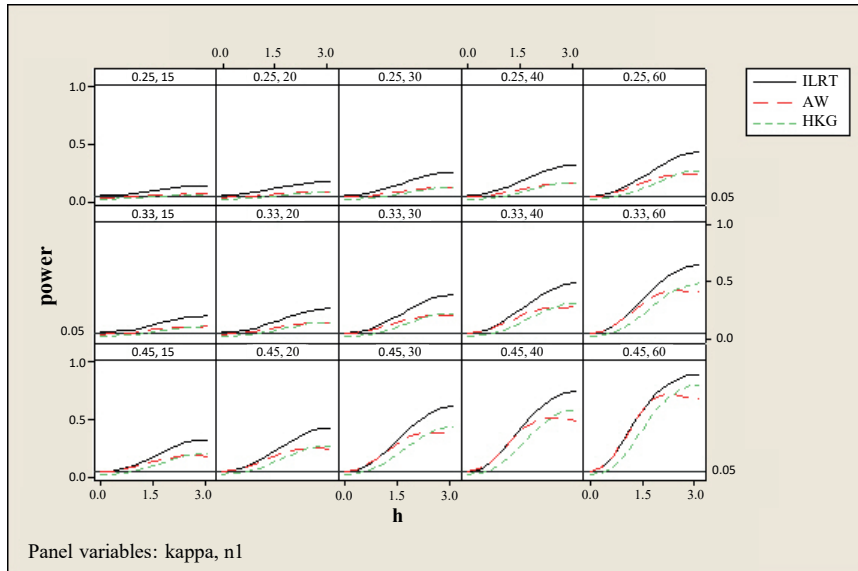


Figure 4. Simulated power functions of ILRT, AW, HKG; two groups and small  $\kappa$ . Panel headings are values of the pairs  $\kappa, n_1$ .

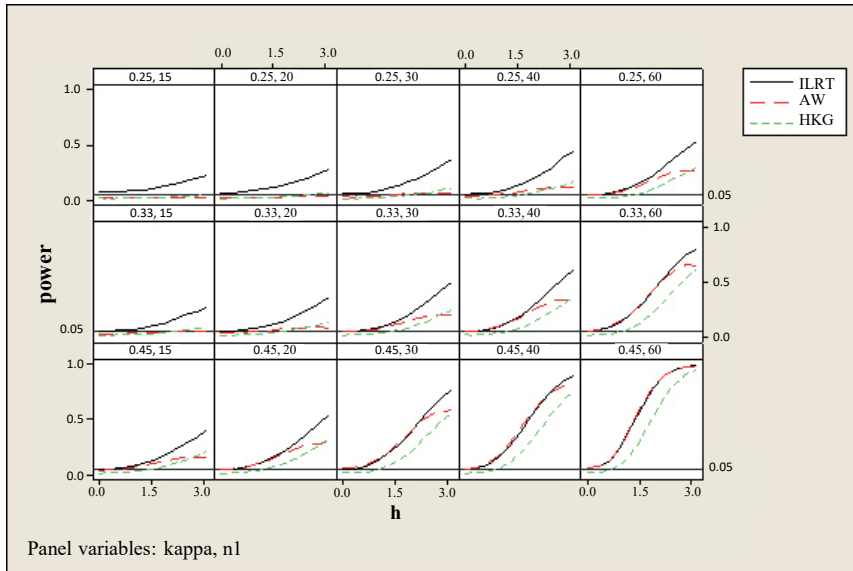


Figure 5. Simulated power functions of ILRT, AW, HKG; eight groups, small  $\kappa$ . Panel headings are values of the pairs  $\kappa, n_1$ .

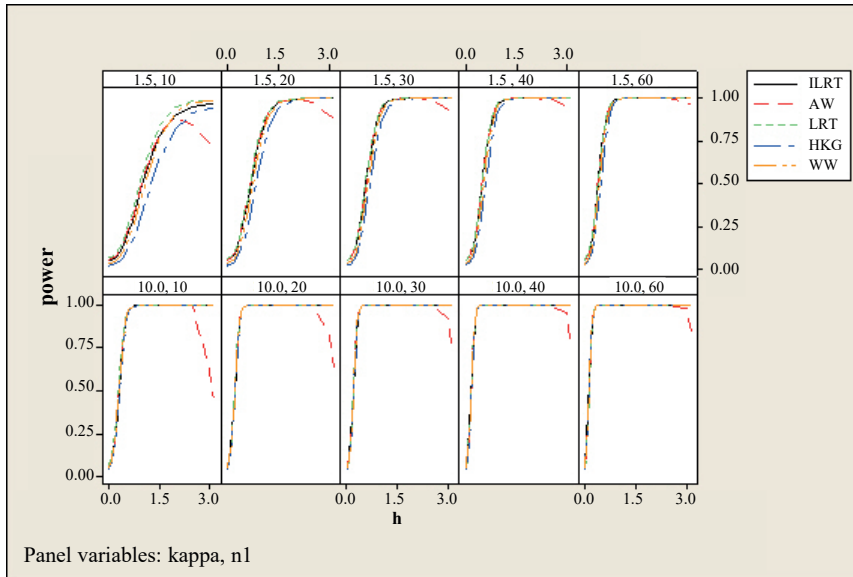


Figure 6. Simulated power functions of ILRT, AW, LRT, HKG, WW; two groups, large  $\kappa$ . Panel headings are values of the pairs  $\kappa, n_1$ .

The only existing test for unknown and unequal concentrations for this problem is the likelihood ratio test suggested by Watson (1983) ( $WW^*$ ), given by

$$T_{WW^*} = 2 \left( \sum_{i=1}^p \hat{\kappa}_i R_i - R_W \right) \sim \chi_{p-1}^2,$$

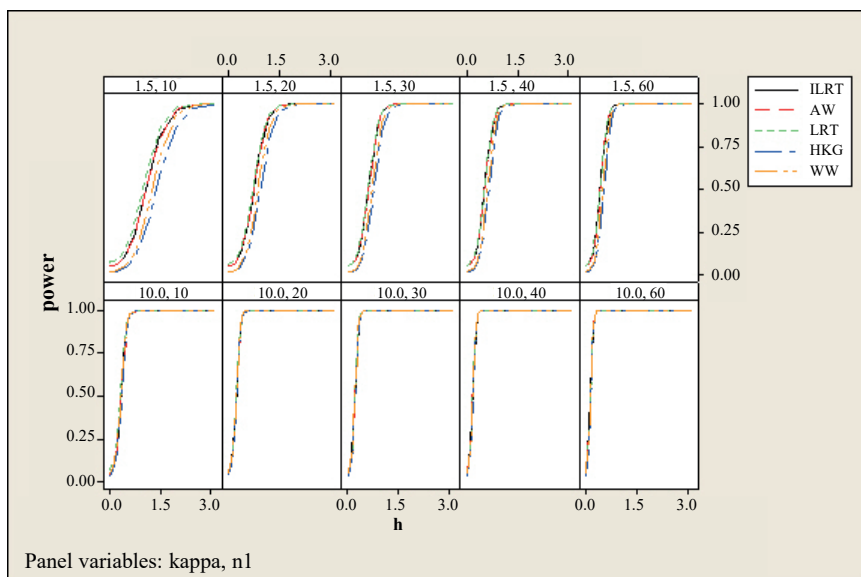


Figure 7. Simulated power functions of ILRT, AW, LRT, HKG, WW; eight groups, large  $\kappa$ . Panel headings are values of the pairs  $\kappa, n_1$ .

where

$$R_W = \left\{ \left( \sum_{i=1}^p \hat{\kappa}_i R_i \cos \theta_i \right)^2 + \left( \sum_{i=1}^p \hat{\kappa}_i R_i \sin \theta_i \right)^2 \right\}^{1/2},$$

where  $\hat{\kappa}_i$  is the MLE of  $\kappa_i$  under the  $i$ th group.

To identify the specific parametric region where an improvement over  $WW^*$  is essential, the power values were simulated using the same setting as those in the case of equal  $\kappa$ . Additionally, increments in the concentration parameters by 0.25 and 0.5 for successive groups were introduced. Though the sizes of actual LRT were unduly large, the size-normalized power function was reasonably good, even for small group sizes. However, size-corrective multiplicative adjustments may depend on the pattern of concentrations across the groups in a complicated way, and thus cannot be derived easily.

The ILRT for this case is developed next. Adopting a parallel approach to that in Section 3.2 with the prior

$$\Pi^*(\boldsymbol{\kappa}) = \prod_{i=1}^p \Pi_i, \quad \Pi_i = (I_0(\kappa_i))^{n_i} \kappa_i^{(n_i-1)/2-1} \exp(-n_i \kappa_i), \quad \kappa_i > 0 \forall i, \quad (4.1)$$

the resulting integrated likelihood function is

$$\bar{L}^*(\boldsymbol{\mu}|\boldsymbol{\theta}) = \prod_{i=1}^p \int L_i \Pi_i d(\kappa_i), \quad (4.2)$$

leading to

$$\bar{L}^*(\boldsymbol{\mu}|\boldsymbol{\theta}) \propto \prod_{i=1}^p [n_i - \sum_{j=1}^{n_i} \cos(\theta_{ij} - \mu_i)]^{-(n_i-1)/2}.$$

The maximizer of  $\bar{L}^*$  with respect to  $\boldsymbol{\mu}$  under  $H_1$  is still  $\bar{\mu}_i^* = \hat{\mu}_i = \theta_i$ , for  $i = 1, \dots, p$ . However, under  $H_0$ ,  $\bar{L}^*$  is maximized at  $\bar{\mu}_0^*$ , which is the solution to the equation

$$\sum_{i=1}^p \frac{S_i \cdot \cos(\bar{\mu}_0^*) - C_i \sin(\bar{\mu}_0^*)}{n_i - C_i \cdot \cos(\bar{\mu}_0^*) - S_i \cdot \sin(\bar{\mu}_0^*)} = 0, \quad (4.3)$$

where  $S_i$  and  $C_i$  are defined in Section 2.1. This leads to the integrated likelihood ratio

$$\bar{\lambda}^* = \prod_{i=1}^p \left[ \frac{n_i - R_i}{n_i - C_i \cdot \cos(\bar{\mu}_0^*) - S_i \cdot \sin(\bar{\mu}_0^*)} \right]^{(n_i-1)/2}.$$

The log likelihood ratio statistic is

$$T_{ILRT}^* = -2 \log \bar{\lambda}^* = \sum_{i=1}^p (n_i - 1) \cdot \log \left( \frac{n_i - R_i}{n_i - C_i \cdot \cos(\bar{\mu}_0^*) - S_i \cdot \sin(\bar{\mu}_0^*)} \right).$$

As before, we have the following result:

**Theorem 2.** *The asymptotic distribution of  $T_{ILRT}^*$  is  $\chi_{p-1}^2$ .*

*Proof of Theorem 2.* Note from equation (11) that

$$\begin{aligned} \bar{L}^*(\boldsymbol{\psi}|\boldsymbol{\theta}) &= \prod_{i=1}^p \int L_i \Pi_i d(\kappa_i) \\ &= \prod_{i=1}^p f_i, \end{aligned}$$

where  $f_i = \int L_i \Pi_i d(\kappa_i)$ . Treating each group separately, and employing similar arguments to those in the proof of Theorem 1 on each  $L_i$  separately, analogues of equations (3.4) through (3.8) hold for each  $f_i$ , such that

$$\begin{aligned} \bar{l}_i(\boldsymbol{\psi}_i) &= \log(f_i) \\ &= l_{A_i}(\boldsymbol{\psi}_i) + \log(\Pi_i(\hat{\kappa}_{i_{\boldsymbol{\psi}_i}})) + \log(g(\hat{\kappa}_{i_{\boldsymbol{\psi}_i}})) + \log(\{1 + O(n^{-1.5})\}), \end{aligned}$$

where  $l_{A_i}(\boldsymbol{\psi}_i)$  is the Cox–Reid adjusted profile likelihood corresponding to  $L_i$ . Taking the logarithms yields

$$\begin{aligned}\bar{l}^*(\boldsymbol{\psi}) &= \sum_{i=1}^p \log(f_i) \\ &= \sum_{i=1}^p l_{A_i}(\boldsymbol{\psi}_i) + \log(\Pi_i(\hat{\kappa}_{i\boldsymbol{\psi}_i})) + \log(g(\hat{\kappa}_{i\boldsymbol{\psi}_i})) + \log(\{1 + O(n^{-1.5})\}).\end{aligned}$$

The MLE(s) of  $\boldsymbol{\mu}$  under  $H_1$  are  $\theta_i$ , as given in Section 2.1, whereas under  $H_0$ , they are  $\bar{\mu}_0^*$ , as given in equation (4.3). The MLEs  $\hat{\kappa}_i$  of  $\kappa_i$  (solutions to the equations  $A(\hat{\kappa}_i) = (R_i)/n_i$ , for  $i = 1, \dots, p$ , where  $R_i$  is defined in Section 2.1) are the same under both  $H_0$  and  $H_1$ . Consequently, the terms containing the estimates of  $\kappa$  in the log likelihood ratio get cancelled out, leaving the following ILRT statistic:

$$-2 \log \bar{\lambda}^* = -2 \sum_{i=1}^p [l_{A_i}(\hat{\boldsymbol{\mu}}) - l_{A_i}(\hat{\boldsymbol{\mu}}_0^*) + O_P(n_i^{-1.5})], \quad (15)$$

Ignoring the  $O_P(n_i^{-1.5})$  terms, and noting the asymptotic  $\chi_1^2$  distribution of the adjusted Cox–Reid likelihood for each group, the additive property of  $\chi^2$  under independence across the groups and a common estimate of the mean under the null establish the asymptotic  $\chi_{p-1}^2$  distribution of  $T_{ILRT^*}$ .

Using the overall sample mean  $\theta_{..}$  in place of  $\bar{\mu}_0^*$  gave a good approximation. In addition, minor fine-tuning with the multipliers 1.085 (for  $0.7 < k_0 < 1$ ), 1.05 (for  $2 < k_0 < 5$ ), and 1.15 (for  $1 < k_0 < 2$ ) further enhanced the size performance. Here,  $k_0$  is the smallest of the estimates of the concentration parameters for the  $p$  groups. Equally good performance was exhibited by the size-adjusted 0.88  $T_{WW^*}$ , with multiplier 0.88 for  $\kappa_0 > 0.7$ . However for very small concentrations, namely  $k_0 < 0.7$ , none of the tests gave satisfactory results. This case requires further investigation.

The next section describes the ILRT for the GvM in the circular case.

#### 4.2. ANOMED for GvM (A case of two nuisance parameters)

Note that the ILRT-based treatment of the nuisance parameter is likely to be more effective under orthogonality between the nuisance parameters and the parameters of interest, and the prior does not depend on the parameters of interest. This fact can be used to construct tests for ANOMED for other dis-

tributions, preferably where the normalizing constant does not depend on the parameter of interest. In this case, its influence can be circumvented by including its reciprocal in the prior, while keeping the prior free of the parameter of interest. These conditions are, for example, satisfied for the three-parameter GvM and Batschelet (1981) distributions, as discussed below. Suppose  $\boldsymbol{\theta} = \{\theta_{ij}, i = 1, \dots, p, j = 1, \dots, n_i\}$  are independent and identically distributed (i.i.d.) observations from the generalized vM distribution, with pdf

$$f(\theta_{ij}) = [2\pi G_0(k_1, k_2)]^{-1} \exp[k_1 \cos(\theta_{ij} - \mu) + k_2 \cos 2(\theta_{ij} - \mu)], k_1 > 0, k_2 > 0,$$

where  $\mu \in [0, 2\pi)$  is a location parameter, and  $G_0(k_1, k_2)$  is the normalizing constant.

The prior  $\Pi(\kappa_1, \kappa_2) = [G_0(\kappa_1, \kappa_2)]^n \exp[-n\kappa_1 - n\kappa_2] k_1^{a_n-1} k_2^{a_n-1}$  is the most appropriate, and yields

$$\bar{L}(\boldsymbol{\mu}|\boldsymbol{\theta}) \propto \left[ n - \sum_i R_i^1 \right]^{a_n} \left[ n - \sum_i R_i^2 \right]^{a_n}, \quad (4.4)$$

where,  $R_i^l(x) = \sum_{j=1}^{n_i} \cos l(\theta_{ij} - x)$ , for  $l = 1, 2$ , leading to the following ILR statistics:

$$T_{GvM\_ILRT} \equiv 2a_n \log \left[ \frac{\left[ n - \sum_i R_i^1(\hat{\mu}_0) \right] \left[ n - \sum_i R_i^2(\hat{\mu}_0) \right]}{\left[ n - \sum_i R_i^1(\hat{\mu}_{1i}) \right] \left[ n - \sum_i R_i^2(\hat{\mu}_{1i}) \right]} \right]. \quad (4.5)$$

Here,  $\hat{\mu}_{1i}$ , for  $i = 1, \dots, p$ , and  $\hat{\mu}_0$  are maximizers of  $\bar{L}(\boldsymbol{\mu})$  under  $H_1$  and  $H_0$ , respectively, and can be obtained using numerical methods. Because the domain of the maximization is bounded, this should not pose much difficulty. The choice of  $a_n$  can be based on the Satterthwaite–Welch-type technique, in line with the arguments in Section 3.2.

A parallel approach holds for the Batschelet (1981) distribution, with density function

$$f(\theta) = C^{-1} \exp[\kappa \cos(\theta - \mu) + \nu \sin(\theta - \mu)]; -\pi \leq \theta, \mu < \pi; \kappa \geq 0; -\infty < \nu < \infty,$$

with  $R_i^2(x)$  replaced by  $\sum_{j=1}^{n_i} \sin(\theta_{ij} - x)$  in equations (4.4) and (4.5). However fine-tuning adjustments described in Section A.1 of Appendix A may need to be developed for small concentrations.

## 5. Examples

This section applies ILRT to real-data examples, representing situations in which ANOMED is most appropriate. The computational details are summarized in Table 1. For WW, HKG, LRT, and AW, the computational formulae given in Section 2.2 are used. The ILRT is computed using equation (3.3), together with the multiplicative correction factor suggested in Section A.1 of Appendix A, where we replace  $\kappa_0$  with its estimate  $\hat{\kappa}_0$ , as reported in Table 1. For the data sets (except data set  $D_3$ , where the raw data were not available), the assumptions of a vM distribution and an equal concentration parameter for the groups were validated (Mardia and Jupp (2000); Fisher (1993)). These examples also demonstrate the proper usage of tests.

### 5.1. Epidemic onset data: D1, D2

In certain epidemic diseases, such as acute primary angle closure glaucoma (APACG), the exact date of attack can be reliably determined. As suggested by Gao et al. (2006) (GAO), each date of onset within a year can be represented as an angle by equating the 365 days of a year to  $360^\circ$  ( $2\pi$  radians). Therefore, one day is equivalent to  $360/365 = 0.986^\circ$ . Then, a well-fitted vM distribution with a single peak (mode) (indicating a prevalent date of onset) would indicate a seasonal influence on such data. Furthermore, note that a significant difference between the peak dates of onset for the groups corresponding to the different levels of an attribute (e.g., age group, gender etc.) indicates an interaction between the seasonal effect and the attribute under consideration.

Gender, adverse environmental conditions, and amount of sunlight are known to be influential factors in causing APACG (Ivanisevic et al. (2002); Hillman and Turner (1977), Sharpec *et al.* (2010)). Because the latter two factors vary with the season, a seasonal impact on the onset of APACG is expected. This may vary by gender and age group, perhaps, owing to differing capabilities of sustaining the adverse conditions.

GAO give data on the exact dates of onset, converted to angles, for 132 APACG patients from Singapore, along with information on other attributes such as age group, gender and so on. The data set D1 is extracted from this database and displays the dates of onset of APACG for male patients, partitioned into four age groups: below 50; 50 to 59; 60 to 69; and above 70. Referring to Table 1 for D1, the estimated concentration under  $H_0$  ( $\hat{\kappa}_0 = 0.2563$ ) is very small, as are the group sizes. Following the recommendations of Section 3.3,

the inference based on the ILRT is the most reliable. The ILRT clearly rejects the hypothesis of no difference (p-value: 0.0151), as did the next favored HKG ((B) (i); Section 3.3) (p-value: 0.0132). This indicates that the seasonal impact varies among the age groups (i.e., the mean dates of onset across the age groups are significantly different). The strength with which WW and LRT rejected the hypothesis (p-value  $< 10^{-3}$ ) is untrustworthy owing to their large type-I errors ((A) (i), Section 3.3), although they do agree with the ILRT. The least powerful test, AW, accepted the null, perhaps incorrectly. Note that in some situations, such a decision could be risky, for example, in case-control studies that assess the effectiveness of a treatment on a gait pattern, under Cerebral Palsy, where even small angular differences with respect to a gait pattern are of great clinical importance.

A similar hypothesis for female patients (data set D2), extracted from the same database under the same age groups, was unanimously accepted by all the tests except WW (which rejected the hypothesis (p-value: 0.0391), conforming to its aforementioned tendency of false alarms under small concentrations). Such a decision can also be undesirable, for example, in drug testing, where falsely declaring a drug to be superior to others could be harmful.

In conclusion, males are prone to age-dependent seasonal effects, whereas seasonal influence does not depend on age for females. This also indicates a three-way interaction between gender, age group and seasonal influence on the dates of onset of APACG. GAO observed such differences, but were not able to establish them statistically using a circular regression, possibly because the interaction effects were not accounted for in their regression model. Further clinical investigation and research is needed in this context, because the results observed here may offer important clues and insights.

## 5.2. Light pulse treatment on the pineal melatonin rhythm: D3

It is widely assumed that the circadian system adapts to local environmental cues, such as light and temperature, which vary enormously across habitats. Moore and Menaker (2012) examined the effect of light pulse treatment on the pineal melatonin rhythm of five *Anolis* lizard species. The data set D3, with small group sizes from a control group and a treatment group, was analyzed in a similar manner to that of the *A. gundlachi* species. As reported in Table 1, the light pulse treatment caused a significant phase delay in the circadian rhythm. This indicates that the circadian system of the species under consideration adapts itself to the light pulse treatment. This is highly concentrated data

Table 1. Computational details for the three data sets.

Data	Group sizes	Resultant lengths	$\hat{\kappa}_0$	p-values
$D_1$ p=4	$n_1 = 5$	$R_1 = 4.0986$	0.2563	ILRT: 0.0151
	$n_2 = 9$	$R_2 = 3.9193$		AW: 0.0869
	$n_3 = 12$	$R_3 = 6.146$		HKG: 0.0132
	$n_4 = 9$	$R_4 = 3.104$		WW: 0.0007
	$N = 35$	$R_0 = 4.4494$		LRT: 0.0007
$D_2$ p=4	$n_1 = 8$	$R_1 = 4.7977$	0.4116	ILRT: 0.1815
	$n_2 = 22$	$R_2 = 3.7932$		AW: 0.1414
	$n_3 = 36$	$R_3 = 6.8435$		HKG: 0.1284
	$n_4 = 31$	$R_4 = 10.7446$		WW: 0.0391
	$N = 97$	$R = 19.5524$		LRT: 0.0923
$D_3$ p=2	$n_1 = 9$	$R_1 = 8.73$	9.0186	ILRT: 0.0006
	$n_2 = 7$	$R_2 = 6.65$		AW: 0.0211; HKG: 0.0154
	$N = 16$	$R = 15.085$		WW: 0.0196; LRT: 0.0115

( $\hat{\kappa}_0 = 9.0176$ ); the analysis as per the recommendations of Section 3.3 ((B) (v), Section 3.3) shows that all tests are equally competent. This is reflected in the unanimous decision to reject the null hypothesis by all tests (all p-values  $< 0.05$ ). However, here too, the ILRT rejects the hypothesis more strongly than the other tests do (p-value = 0.0006), favoring the conjectured behavior.

## 6. Conclusion

Our motivation for this study was to develop an efficient parametric test for the homogeneity of the mean directions of several independent circular populations, which can be universally implemented in practice. The need for such a test emerged from the fact that there is no universal test in the existing literature that shows acceptable performance and can be applied to diverse realistic situations, for example low concentrations and a large number of small size groups. We have derived a universal, yet simple and elegant test statistic. We have demonstrated that our method can be extended in a straightforward manner to a rich class of distributions, including asymmetric, bimodal, sharply peaked, and flat-topped distributions among others, as modeled by, for example generalized vM and Batschelet distributions. The difficulty of the non-location-scale nuisance parameters  $\kappa$  was overcome by introducing a new approach based on the integrated likelihood ratio test. Furthermore, extensive simulations showed that our test outperforms existing tests in the usual parametric region, and com-

petes uniformly well with the best of these other tests. Finally, our approach is amenable to elegant and almost straightforward generalizations to higher dimensions (i.e., to hyper-spherical, e.g., Langevin, populations). This last observation is currently being studied further.

## Acknowledgements

Part of this work was completed by Prof. Ashis SenGupta as Distinguished Professor at Middle East Technical University, Ankara, Turkey. A major part of this work was completed during the visits of Dr. H. V. Kulkarni to ASU, Indian Statistical Institute, Kolkata, India (ISI). She was partially supported by ISI, The National Board for Higher Mathematics (NBHM), Department of Atomic Energy (DAE), India, under Grant no. 2/48(34)/2016/NBHM(RP)/R&D II/4531; by the Department of Science and Technology (DST) under Grant SR/FST/MSI-103, dated November 18, 2015; and, UGC, New Delhi under UGC-SAP Grant F.520/8/DRS-I/2016 (SAP-I) dated 8th March 2016, awarded to the Department of Statistics, Shivaji University, Kolhapur, for financial support.

Lastly, we thank an anonymous referee for his/her careful reading and valuable suggestions.

## A. Appendix

### A.1. Corrective adjustments for small concentrations

The corrective multiplicative adjustment  $cf_{ILrt}$  given below for controlling the sizes of ILRT under small and equal concentrations was derived by regressing the ratio of theoretical 95<sup>th</sup> quantile of the desired  $\chi_{p-1}^2$  distribution to the simulated 95<sup>th</sup> quantiles of  $T_{ILRT}$  under  $H_0$  based on 200,000 simulations. A large number of parametric combinations of input parameters  $n$ ,  $p$  and  $\kappa$  were used and then  $\kappa$  was replaced by its estimate  $\hat{\kappa}_0$ . The densely clustered sizes around the target level of the multiplicatively adjusted ILRT as seen in the corresponding box-plot in Figure 1 are indicative of a closer conformation to the desired  $\chi_{p-1}^2$  distributional assumption.

$$cf_{ILrt} = \begin{cases} 0.563 - 0.0029.n_1 + 0.029p + 0.93.\kappa_0 - 0.32.\sqrt{p} \\ -0.12 \log(N) + 0.32. \log(p) - 0.186. \log(\kappa_0) + 0.019n_1.\kappa_0 & \text{if } \kappa_0 < 0.4, \\ (1.92 - 0.0186\sqrt{p} + 0.0544 \log(N) - 0.985\sqrt{\kappa_0} + \log(\kappa_0) \\ -0.002.\sqrt{N} + 0.001.n_1 - 0.01\sqrt{n_1}). & \text{if } 0.4 < \kappa_0 < 1. \end{cases}$$

Table 2. Details of the piece-wise approximation  $c + b\omega$ ,  $\omega = 1/\kappa$  for  $A(\kappa)$ .

Domain for $\kappa$	$c$	$b$
[ 1 , 1.45)	0.391	1.84
[ 1.45, 3 )	0.235	1.95
[ 3 , 4.25)	0.149	1.98
[ 4.25, 10 )	0.0805	1.99
[10 , 15 )	0.046	2
[15 , 50 )	0.0181	2
>50	0.007	2

Furthermore, as mentioned in the proof of Theorem 1 a little fine-tuning for moderate values of  $\kappa \in (1, 9)$  namely, 1.11 for  $\{1 < \kappa_0 < 1.25\} \cup \{3 < \kappa_0 < 4.25\}$ ; 1.17 for  $1.25 < \kappa_0 < 3$ ; 1.04 for  $4.25 < \kappa_0 < 9$  gave excellent results. Also for  $\kappa_0 > 15$ ,  $a_n = n - 1.5$  in place of  $n - 1$  gave more accurate results.

A.2 Piece-wise approximation of  $A(\kappa)$ :

Note that for  $\kappa \in [1, \infty)$ ,  $\omega = 1/\kappa \in (0, 1]$ . By computing  $A(\omega)$  on a very fine mesh of  $(0, 1]$  and regressing  $A(\omega)$  versus  $\omega$  piece-wise on the partition given in Table 2, (chosen selectively) the approximation of  $A(\kappa)$  with error less than  $10^{(-3)}$  reported in Table 2 was obtained.

## References

- Anderson, C. M. and Wu, C. F. (1995). Measuring location effects from factorial experiments with a directional response. *Int. Statist. Review* **63**, 345-363.
- Batschelet, E. (1981). Circular statistics in biology **Vol. 111**. London: Academic Press.
- Beran, R. and Fisher, N. I. (1998). Nonparametric comparison of mean directions or mean axes. *The Ann. Statist.* **26**, 472-493.
- Berger, J. O., Liseo, B. and Wolpert, R. (1999). Integrated likelihood functions for eliminating nuisance parameters (with discussion). *Statist. Sci.* **14**, 1-28.
- Chamberlain, G. (2007). Decision theory applied to an instrumental variables model. *Econometrica* **75**, 609-652.
- Cox, D. R. and Reid, N. (1987). Parameter orthogonality and approximate conditional inference. *J. R. Stat. Soc. Ser. B. Stat. Methodol.* **49**, 1-39.
- Fisher, N. I. (1993). *Statistical Analysis of Circular Data*. Cambridge, MA: Cambridge University Press.
- Gao, F., Chia, K. S., Krantz, I., Nordin, P. and Machin, D. (2006). On the application of the von Mises distribution and angular regression methods to investigate the seasonality of disease onset. *Statist. in Medicine* **25**, 1593-1618.
- Ghosh, M., Datta, G. S., Kim, D. and Sweeting, T. J. (2006). Likelihood-based inference for ratios of regression coefficients in linear models. *Ann. of the Institute of Statist. Mathematics* **58**, 457-473.
- Hillman, J. S., and Turner, D. C. (1977). Association between acute glaucoma and the weather

- and sunspot activity. *Brit. J. of Ophthalmology* **249**, 223-233.
- Ivanisevic, M., Erceg, M., Smoljanovic, A. and Trosic, Z. (2002). The incidence and seasonal variations of acute primary angle-closure glaucoma. *Collegium Antropologicum* **1**, 41-45.
- Jammalamadaka, S. R. and SenGupta, A. (2001). *Topics in Circular Statistics*. USA: World Scientific.
- Kalbfleisch, J. D. and Sprott, D. A. (1970). Application of likelihood methods to models involving large numbers of parameters (with discussion). *J. R. Stat. Soc. Ser. B. Stat. Methodol.* **32**, 175-208.
- Larsen, P. V., Blaesild, P. and Sorensen, M. K. (2002). Improved likelihood ratio tests on the von Mises-Fisher distribution. *Biometrika* **89**, 947-951.
- Liseo, B. (1993). Elimination of nuisance parameters with reference priors. *Biometrika* **80**, 295-304.
- Lozano, Y. R. (2016). *Landmark Processing by Head Direction Cells*. Diss. UCL (University College London).
- Malley, J. D., Redner, R. A., Severini, T. A., Badner, J. A., Pajevic, S. and Bailey-Wilson, J. E. Estimation of linkage and association from allele transformation data. *Biometrical Journal* **45**, 349-366.
- Mardia, K. V. and Jupp, P. E. (2000). *Directional Statistics*. Willy Series in Probability and Statistics.
- Moore, A. F. and Menaker, M. (2012). Photic resetting of the circadian clock is correlated with photic habitat in Anolis lizards. *J. of Comparative Physiology A* **198**, 375-387.
- SenGupta, A. and Roy, R. (2011). Testing homogeneity of mean directions for circular dispersion models. *Calcutta Statistical Association Bulletin (Special 7-th Triennial Proceedings Volume)* **63**, 249-263.
- Severini, T. A. (2007). Integrated likelihood functions for non-Bayesian inference. *Biometrika* **94**, 529-542.
- Severini, T. A. (2010). Likelihood ratio statistics based on an integrated likelihood. *Biometrika* **97**, 481-496.
- Severini, T. A. (2011). Frequency properties of inferences Based on an integrated likelihood function. *Statistica Sinica* **21**, 433-447.
- Shay, C. F., Ferrante, M., Chapman IV, G. W. and Hasselmo, M. E. (2016). Rebound spiking in layer II medial entorhinal cortex stellate cells: possible mechanism of grid cell function. *Neurobiology of Learning and Memory* **129**, 83-98.
- Stephens, M. A. (1972). Multisample tests for the von Mises distribution. *J. Am. Stat. Asso.* **67**, 456-461.
- Watson, G. S. (1983). Large sample theory of the Langevin distribution. *Journal of Statistical Planning and Inference* **8**, 245-256.
- Watson, G. S. and Williams, E. J. (1956). On the construction of significance tests on the circle and the sphere. *Biometrika* **43**, 344-352.

Indian Statistical Institute, Kolkata, WB 700108, India.

Augusta University, Augusta, GA 30912, USA.

E-mail: amsseng@gmail.com

Department of Statistics, Shivaji University, Kolhapur, India, 416004.

E-mail: kulkarni.hemangi@gmail.com

(Received November 2017 ; accepted November 2018)